Probing Chitosan and Phospholipid Interactions Using Langmuir and Langmuir−Blodgett Films as Cell Membrane Models

Felippe J. Pavinatto,[†] Luciano Caseli,*[,†] Adriana Pavinatto,[†] David S. dos Santos, Jr.,[‡] Thatyane M. Nobre,[§] Maria E. D. Zaniquelli,[§] Heurison S. Silva,[†] Paulo B. Miranda,[†] and Osvaldo N. de Oliveira, Jr.[†]

Grupo de Polímeros Bernhard Gross, Instituto de Física de São Carlos (IFSC), Universidade de São Paulo, Avenida Trabalhador São Carlense 400, CEP 13560-970, Centro, São Carlos-SP, Brazil, Materials & Surface Science Group, University of Windsor, Windsor, Ontario, Canada, and Departamento de Química, Faculdade de Filosofia, Ciências e Letras de Ribeirão Preto, Universidade de São Paulo, Ribeirão Preto-SP, Brazil

Received March 23, 2007. In Final Form: April 25, 2007

The interaction between chitosan and Langmuir and Langmuir−Blodgett (LB) films of dimyristoyl phosphatidic acid (DMPA) is investigated, with the films serving as simplified cell membrane models. At the air−water interface, chitosan modulates the structural properties of DMPA monolayers, causing expansion and decreasing the monolayer elasticity. As the surface pressure increased, some chitosan molecules remained at the interface, but others were expelled. Chitosan could be transferred onto solid supports alongside DMPA using the LB technique, as confirmed by infrared spectroscopy and quartz crystal microbalance measurements. The analysis of sum-frequency vibration spectroscopy data for the LB films combined with surface potential measurements for the monolayers pointed to chitosan inducing the ordering of the DMPA alkyl chains. Furthermore, the morphology of DMPA LB films, studied with atomic force microscopy, was affected significantly by the incorporation of chitosan, with the mixed chitosan−DMPA films displaying considerably higher thickness and roughness, in addition to chitosan aggregates. Because chitosan affected DMPA films even at pressures characteristic of cell membranes, we believe this study may help elucidate the role of chitosan in biological systems.

Introduction

Cell membranes can be considered as two weakly coupled monolayers, which has motivated the use of Langmuir monolayers as a membrane model,[1] especially because interactions between biological species can be studied in two dimensions with easy control of lateral pressure, molecular density, and composition. In addition to the Langmuir monolayers, deposited Langmuir−Blodgett (LB) films[22] may be used to mimic highly organized lamellar lipid stacking, which can also be applied in biosensors,[3] bioreactors,[4]and electrical and photodevices.[5,6] A variety of biologically relevant molecules have already been studied in Langmuir and LB films containing phospholipids.[7−9] Of particular interest for this work is chitosan, a natural polysaccharide extracted from chitin,[10] which has been used for a number of applications,[11,12] including use as a weight-reducing agent,[13] nanoparticle synthesis,[14,15] and in drugs and gene delivery,[16,17] because of its biocompatibility, biodegradability, and low cytotoxicity.[11,18]

Chitosan interacts with liposomes[19,20] and other mimetic systems,[21] but few studies exist about its interaction with Langmuir and LB films.[22,23] It is important to understand how chitosan interacts with cell membrane models because of its properties as a bactericide agent, and for medical applications, including use of liposomes in drug delivery. Moreover, the action of chitosan as a weight reducer involves lipid−polysaccharide interactions. Although chitosan has negligible surface activity,[24] it adsorbs on

* Corresponding author. Telephone: 55 16 3373-8061. Fax: 55 16 3371-5365. E-mail: lcaseli@usp.br.

[†] Instituto de Física de São Carlos (IFSC), Universidade de São Paulo.

[‡] University of Windsor.

[§] Faculdade de Filosofia, Ciências e Letras de Ribeirão Preto, Universidade de São Paulo.

(1) Brockman, H. *Curr. Opin. Struct. Biol.* **1999**, *9*, 438−443.

(2) Roberts, G. *Langmuir-Blodgett Films*; Plenum Press: New York, 1990.

(3) Caseli, L.; Moraes, M. L.; Zucolotto, V.; Ferreira, M.; Nobre, T. M.; Zaniquelli, M. E. D.; Rodrigues, U. P.; Oliveira, O. N. *Langmuir* **2006**, *22*, 8501−8508.

(4) Wan, K.; Chovelon, J. M.; Jaffrezic-Renault, N. *Talanta* **2000**, *52*, 663−670.

(5) Oliveira, O. N., Jr.; dos Santos, D. S., Jr.; Balogh, D. T.; Zucolotto, V.; Mendonca, C. R. *Adv. Colloid Interface Sci.* **2005**, *116*, 179−192.

(6) Oliveira, O. N., Jr.; He, J.-A.; Zucolotto, V.; Balasubramanian, S.; Li, L.; Nalwa, H. S.; Kumar, J.; Tripathy, S. K. Layer-by-Layer Polyelectrolyte-Based Thin Films for Electronic and Photonic Applications. In *Handbook of Polyelectrolytes and Their Applications*; Tripathy, S. K., Kumar, J., Nalwa, H. S., Eds.; American Scientific Publishers: Stevenson Ranch, CA, 2002.

(7) Leblanc, R. M. *Curr. Opin. Chem. Biol.* **2006**, *10*, 529−536.

(8) Girard-Egrot, A. P.; Godoy, S.; Blum, L. J. *Adv. Colloid Interface Sci.* **2005**, *116*, 205−225.

(9) Brezesinski, G.; Mohwald, H. *Adv. Colloid Interface Sci.* **2003**, *100−102*, 563−584.

(10) Tharanathan, R. N.; Kittur, F. S. *Crit. Rev. Food Sci. Nutr.* **2003**, *43*, 61−87.

(11) Onishi, H.; Machida, Y. *Biomaterials* **1999**, *20*, 175−182.

(12) Thakkar, H.; Sharma, R. K.; Mishra, A. K.; Chuttani, K.; Murthy, R. S. R. *J. Pharm. Pharmacol.* **2004**, *56*, 1091−1099.

(13) Furda, I. United States Patent No. 4,233,023, 1980.

(14) Fernandes, A. L. P.; Morais, W. A.; Santos, A. I. B.; de Araujo, A. M. L.; dos Santos, D. E. S.; dos Santos, D. S.; Pavinatto, F. J.; Oliveira, O. N.; Dantas, T. N. C.; Pereira, M. R.; Fonseca, J. L. C. *Colloid Polym. Sci.* **2005**, *284*, 1−9.

(15) Li, M. G.; Lu, W. L.; Wang, J. C.; Zhang, X.; Zhang, H.; Wang, X. Q.; Wu, C. S.; Zhang, Q. *J. Nanosci. Nanotechnol.* **2006**, *6*, 2874−2886.

(16) Salmaso, S.; Bersani, S.; Semenzato, A.; Caliceti, P. *J. Nanosci. Nanotechnol.* **2006**, *6*, 2736−2753.

(17) Prego, C.; Torres, D.; Alonso, M. J. *J. Nanosci. Nanotechnol.* **2006**, *6*, 2921−2928.

(18) Oliveira, I. R. W. Z.; Vieira, I. C. *Quim. Nova* **2006**, *29*, 932−939.

(19) Fang, N.; Chan, V.; Mao, H. Q.; Leong, K. W. *Biomacromolecules* **2001**, *2*, 1161−1168.

(20) Mertins, O.; Cardoso, M. B.; Pohlmann, A. R.; da Silveira, N. P. *J. Nanosci. Nanotechnol.* **2006**, *6*, 2425−2431.

(21) Kaladhar, K.; Sharma, C. P. *Langmuir* **2004**, *20*, 11115−11122.

(22) Pavinatto, F. J.; Santos, D. S. d., Jr., Oliveira, N. O. *Polím.: Ciênc. Tecnol.* **2005**, *15*, 91−94.

(23) Parra-Barraza, H.; Burboa, M. G.; Sanchez-Vazquez, M.; Juarez, J.; Goycoolea, F. M.; Valdez, M. A. *Biomacromolecules* **2005**, *6*, 2416−2426.

(24) Sui, W. P.; Song, G. L.; Chen, G. H.; Xu, G. Y. *Colloids Surf., A: Physicochem. Eng. Aspects* **2005**, *256*, 29−33.

10.1021/la700856a CCC: $37.00
Published on Web 06/01/2007

lipid monolayers and changes their organization. What is still in doubt is whether chitosan remains at the interface at high surface pressures. In this work, we investigate the interaction of chitosan with dimyristoyl phosphatic acid (DMPA) monolayers, with particular emphasis on how chitosan can change the packing and ordering of the films. DMPA was used because of the easiness to transfer this lipid as LB films and because we can extrapolate the results to other negative phospholipids. The measurements involve surface pressure and surface potential−area isotherms and dynamic surface elasticity with the pendant drop technique. The presence of chitosan at high surface pressures is confirmed by transferring mixed chitosan−lipid monolayers onto solid supports using the LB technique. The LB films are characterized with a quartz crystal microbalance (QCM), atomic force microscopy (AFM), infrared and sum-frequency generation (SFG) spectroscopies. Taking all the data together, we propose a model for the location and interaction of chitosan in the DMPA films.

Materials and Methods

Dimyristoyl phosphatidic acid (DMPA) was purchased from Sigma Chemical Co. and used as received. Chitosan was obtained from the deacetylation of chitin extracted from the shells of shrimps,[25] with a degree of acetylation of 15%, as determined using hydrogen nuclear magnetic resonance according to the method of ref 25. The molecular weight, M_n (108 700 Da), and polydispersity index (6.2) were determined by size exclusion chromatography (SEC). Langmuir and LB films were fabricated with a mini-KSV Langmuir trough housed in a class 10 000 clean room. The trough is equipped with a surface pressure sensor (Wilhelmy method) and a Kelvin probe to measure surface potential. Aliquots of a chloroform (Mallinckrodt) DMPA solution (0.5−1.0 mg mL^{-1}) were spread on an aqueous subphase containing Theorell−Stenhagen buffer (NaOH, citric acid, boric acid, phosphoric acid, the pH of which was adjusted to 3.0 with the addition of 2 mol L^{-1} HCl). Water for preparing the buffer solution was supplied by a Milli-RO coupled to a Milli-Q purification system from Millipore (resistivity 18.2 MΩ·cm, pH ∼ 6). The chitosan samples were dissolved in the buffer mentioned, using concentrations varying between 0.050 and 0.200 mg mL^{-1}, and employed as the subphase for lipid monolayers. The ionic strength was kept at 0.03 mol L^{-1}, at which chitosan is believed to adopt a random coil conformation.[26] Compression was performed with a speed of 5 $Å^2$ $molecule^{-1}$ min^{-1} using movable barriers. Surface pressure−area (π−A) and surface potential−area (ΔV−A) isotherms were measured simultaneously at 23 ± 1 °C. From the surface pressure isotherms, we obtained the surface compressional moduli, Cs^{-1}, defined as $-A(\partial\pi/\partial A)$ and also referred to as in-plane elasticity,[27] where A is the mean molecular area, and π is the surface pressure.

The dynamic elasticity for DMPA and mixed chitosan−DMPA monolayers, with several lipid packing densities (corresponding to different initial surface pressures), was studied with the axisymmetric shape drop analysis method (OCA-20 from Dataphysics Instruments GmbH, Germany), with oscillating drop accessory ODG-20, as described in refs 28 and 29 In this measurement, a chloroform solution of ca. 10^{-4} mol L^{-1} of DMPA was gently touched on the surface of a reduced size drop, which was formed with the buffer solution, with or without chitosan. The drop was then rapidly expanded up to a predetermined drop area rendering the desired surface pressure. The dynamic surface elasticity data were obtained after the surface tension reached a constant value by using a periodic drop oscillation with an amplitude of 0.1 mm (relative area variation $\Delta A/A = 5.5\%$) and a frequency of 1.0 Hz. The viscous effect, related to the imaginary part of the elasticity modulus, was estimated from the phase angle.

The transfer of DMPA or chitosan−DMPA monolayers onto solid supports was performed at a constant surface pressure of 40 mN m^{-1}, a temperature of 23 ± 1 °C, and a deposition rate of 5.0 mm min^{-1}. For mixed chitosan−DMPA monolayers, the polysaccharide solution concentration was 0.2 g L^{-1}. The supports used were CaF_2 for infrared spectroscopy, AT-cut quartz crystal coated with Au (Stanford Research Systems, Inc.) with a fundamental frequency of ca. 5 MHz for QCM nanogravimetry, mica for AFM measurements, and infrared-grade fused silica for SFG spectroscopy. Eleven-layer Y-type LB films were built with control of the transfer ratio during each deposition. The first layer was deposited during the upstroke, and 30 min elapsed to allow the film to dry before transferring the second layer (downstroke). The presence of both lipid and chitosan in the LB films was inferred by transmission Fourier transform infrared spectroscopy (FTIR, Thermo Nicolet Nexus 470) and a QCM (Stanford Research Systems, Inc.). To evaluate the morphology of the films, AFM images were obtained in the tapping mode, employing a resonance frequency of approximately 300 kHz, a scan rate of 1.0 Hz, and scanned areas of 10 × 10 μm, 5 × 5 μm and 1 × 1 μm, using a Digital AFM-Nanoscope IIIa instrument. The tip was made from silicon. Film thickness was estimated by producing a furrow on the film with the AFM tip that was made to scan the sample along the same line several times with increased forces until the substrate was touched, as described in ref 30. The film thickness was then obtained from the depth profile across the furrow for LB films with one layer and five layers.

The structuring of DMPA in LB films was studied with SFG, which is sensitive to conformation and molecular ordering by selection rules of the nonlinear susceptibility at interfaces. Here, we briefly describe the main concepts of SFG, and a detailed theory can be found elsewhere.[31] Two input laser beams at frequencies ω_{vis} and ω_{IR} overlap at an interface and generate an output at frequency $\omega_{SFG} = \omega_{vis} + \omega_{IR}$. The signal is proportional to the square of the nonlinear susceptibility $\chi_s^{(2)}(\omega_{SFG} = \omega_{vis} + \omega_{IR})$. As a second-order process, it is forbidden in media with inversion symmetry within the electric-dipole approximation, but allowed at interfaces where the inversion symmetry is broken. That is the reason why SFG can detect only molecules at interfaces, discriminating them from bulk species. When ω_{IR} approaches a vibrational resonance, the SFG output is resonantly enhanced, yielding a surface vibrational spectrum. SFG is therefore able to nonintrusively monitor the structure and packing of Langmuir and LB[32] films. It has been shown, for instance, that the CH-stretch region of the SFG spectra is very sensitive to alkyl chain conformation.[33,34] We used a commercial SFG spectrometer (Ekspla, Lithuania). A pulsed Nd^{+3}:YAG laser provides a fundamental beam at 1064 nm (28 ps pulse duration, 20 Hz repetition rate), with an harmonic unit generating second and third harmonics (532 and 355 nm, respectively). The first is the visible beam that excites the sample (pulse energy ∼ 950 μJ). The third harmonic and fundamental beams pump an optical parametric amplifier with a difference-frequency stage that generates an infrared (IR) beam tunable from 1000 to 4000 cm^{-1} (pulse energy ∼ 30−150 μJ), which overlaps the visible beam on the sample. The incidence angles and approximate spot sizes on the sample are 51°, 500 μm and 60°, 1000 μm for the IR and visible beams, respectively. The sum-frequency signal as a function of IR frequency is collected by a photomultiplier after spatial and spectral filtering. For each scan, data are collected with 100 shots/data point in 3 cm^{-1} increments.

(25) Signini, R.; Campana, S. P. *Polym. Bull.* **1999**, *42*, 159−166.
(26) Tsaih, M. L.; Chen, R. H. *J. Appl. Polym. Sci.* **1999**, *73*, 2041−2050.
(27) Davies, J. T.; Rideal, E. K. *Interfacial Phenomena*, 2nd ed; Academic Press: New York, 1963.
(28) Caseli, L.; Masui, D. C.; Furriel, R. P. M.; Leone, F. A.; Zaniquelli, M. E. D. *J. Braz. Chem. Soc.* **2005**, *16*, 969−977.
(29) Nobre, T. M.; Wong, K.; Zaniquelli, M. E. D. *J. Colloid Interface Sci.* **2007**, *305*, 142−149.
(30) Lobo, R. F. M.; Pereira-da-Silva, M. A.; Raposo, M.; Faria, R. M.; Oliveira, O. N. *Nanotechnology* **1999**, *10*, 389−393.
(31) Lambert, A. G.; Davies, P. B.; Neivandt, D. J. *Appl. Spectrosc. Rev.* **2005**, *40*, 103−145.
(32) Nickolov, Z. S.; Britt, D. W.; Miller, J. D. *J. Phys. Chem. B* **2006**, *110*, 15506−15513.
(33) Ma, G.; Allen, H. C. *Photochem. Photobiol.* **2006**, *82*, 1517−1529.
(34) Guyotsionnest, P.; Hunt, J. H.; Shen, Y. R. *Phys. Rev. Lett.* **1987**, *59*, 1597−1600.

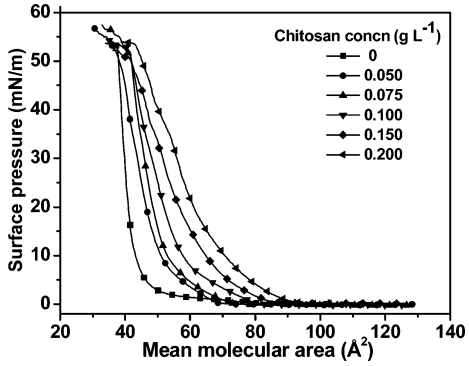

Figure 1. Surface pressure−area (π−A) isotherms for DMPA with several chitosan concentrations in the subphase.

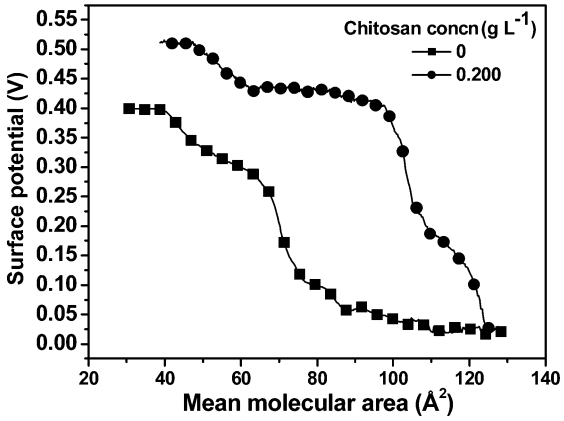

Figure 2. Surface potential−area (ΔV−A) isotherms for DMPA spread on a buffer subphase (squares) and on a 0.200 g L^{-1} chitosan buffer solution subphase (circles).

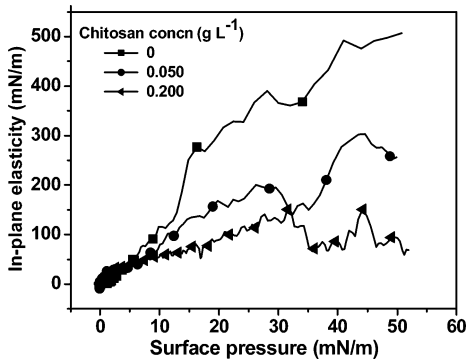

Figure 3. Effect of chitosan on in-plane elasticity of DMPA monolayers, with elasticity plotted vs surface pressure for DMPA monolayers spread onto subphases with two concentrations of chitosan and pure DMPA.

Results and Discussion

(A) Langmuir Monolayers. Figure 1 shows the surface pressure−area isotherms for pure DMPA and mixed chitosan−DMPA monolayers. For the pure lipid, the surface pressure increases slowly to 1−2 mN m^{-1} up to a compression of ca. 50 $Å^2$, after which a liquid-condensed state is reached with collapse at 54 mN m^{-1}. The minimum area, taken as the extrapolation of the more-condensed state to a nil surface pressure, is 41 $Å^2$, consistent with the literature.[35] For the concentration range used in the subphase (0.05−0.2 g L^{-1}), chitosan is not surface-active, and no change in pressure was observed when the barriers in the Langmuir trough compressed the chitosan solution surface. The lack of surface activity has been attributed to the poor amphiphilicity of chitosan,[36] although some activity may appear at high concentrations (e.g., 0.75 g L^{-1}), depending on factors such as acetylation degree, average molecular weight, and polydispersity.[36] Chitosan presents low surface activity, but it can enhance its surface adsorption when mixed with surfactants,[37−39] or when there is a lipid monolayer at the interface.[40] This is clearly shown in Figure 1, in which we can observe that increasing concentrations of chitosan in the subphase led to an increasing expansion of DMPA monolayers. A similar effect from chitosan was observed for cholesterol,[22,23] stearic acid,[23] and DPPC and DPPG[40] monolayers. Note that, at high surface pressures, the expansion due to chitosan is smaller, as if it were being expelled from the interface.

The expansion of the monolayer due to chitosan was also manifested in the surface potential isotherms shown in Figure 2. For pure DMPA, the surface potential is zero at large areas per molecule because of charge neutralization at low pH (∼3). At higher pHs, the surface potential is negative at large molecular areas due to the dissociation of phosphate acid groups. The maximum surface potential was 0.4 V. With the introduction of chitosan in the subphase, the maximum surface potential increased to ca. 0.5 V. The increase could be caused by a combination of factors, such as alteration of the average vertical component of the dipole moment of phospholipid molecules (tilted in relation to the interface), the effect of surface charge altering the arrangement of water molecules near the interface, and the dipole moment of chitosan. We shall return to this point while discussing the SFG data for the LB films.

Chitosan caused the in-plane elasticity (also known as the compressional modulus) of DMPA monolayers to decrease, as shown in Figure 3.

This parameter is often used to characterize monolayer fluidity correlated with phase behaviors.[41] A compressional modulus between 100 and 250 mN m^{-1} is characteristic of the liquid-condensed phase, while a value of Cs^{-1} between 10 and 100 mN m^{-1} denotes the liquid-expanded phase.[27] The monolayer elasticity decreased at all surface pressures, indicating the presence of a new and "soft" component (chitosan) at the interface. The monolayer expansion and decrease in surface elasticity due to chitosan are better visualized in Figure 4.

Table 1 shows the results for the dynamic surface elasticity (ϵ) for DMPA monolayers formed on a drop of buffer or chitosan-containing buffer. The dynamic elasticity measured after the adsorption equilibrium for DMPA monolayers decreased with the incorporation of chitosan for all surface pressures studied, with a maximum decrease of ca. 13% for the highest surface pressure. Although the change in the elasticity modulus was small, larger changes were observed in the phase angle, which accounts for the imaginary contribution for elasticity. For a surface pressure of 5 mN/m, the phase angle was more than 3 times the value measured in the absence of chitosan. It is accepted that an effective viscosity calculated from the imaginary part of elasticity

(35) Losche, M.; Helm, C.; Mattes, H. D.; Mohwald, H. *Thin Solid Films* **1985**, *133*, 51−64.
(36) Qun, G.; Ajun, W. *Carbohydr. Polym.* **2006**, *64*, 29−36.
(37) Babak, V. G.; Vikhoreva, G. A.; Anchipolovsky, M. A. *Mendeleev Commun.* **1996**, *6*, 73−75.
(38) Babak, V. G.; Vikhoreva, G. A.; Lukina, I. G. *Colloids Surf., A: Physicochem. Eng. Aspects* **1997**, *128*, 75−89.
(39) Babak, V.; Lukina, I.; Vikhoreva, G.; Desbrieres, J.; Rinaudo, M. *Colloids Surf., A: Physicochem. Eng. Aspects* **1999**, *147*, 139−148.
(40) Pavinatto, F. J.; Pavinatto, A.; Caseli, L.; dos Santos, D. S., Jr.; Nobre, T. M.; Zaniquelli, M. E. D.; Oliveira, O. N., Jr. *Biomacromolecules* **2007**, *8*, 1633−1640.
(41) Johansson, T. P.; Leach, G. W. *J. Phys. Chem. B* **2006**, *110*, 16567−16574.

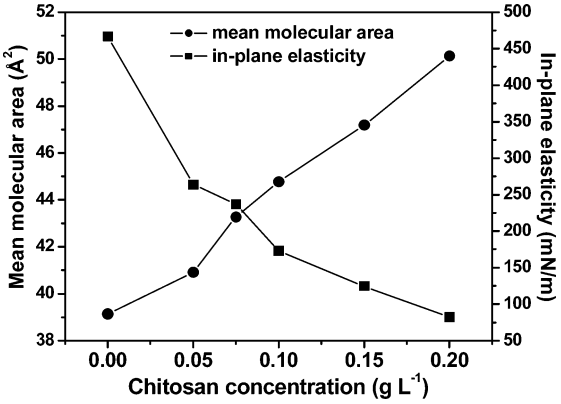

Figure 4. Effect of chitosan concentration on DMPA monolayers in terms of expansion and elasticity changes at a surface pressure of 40 mN m^{-1}.

Table 1. Dynamic Surface Viscoelastic Properties for DMPA and Mixed Chitosan−DMPA Monolayers Obtained with the Axisymmetric Drop Shape Analysis

π (mN/m)	$\epsilon \pm 0.5$ (mN/m)		phase angle (°)	
DMPA	DMPA	DMPA + chitosan	DMPA	DMPA + chitosan
5	20.4	18.8	3.0	10.1
15	48.1	44.9	5.1	10.7
30	79.4	68.3	6.8	11.1

should be related to dissipative and diffusive processes (see ref 42 for a discussion of controversies about this issue). The viscous effect promoted by chitosan is more relevant at low surface pressure when the phospholipid chains are far apart from each other. On the other hand, at higher surface packing with significant short-range interactions, the elastic contribution of the phospholipid monolayer dominates. In summary, the adsorption of chitosan changed the monolayer elasticity in both cases: under quasi-equilibrium conditions (Figures 3 and 4) and under dynamic conditions (Table 1).

Since a cell membrane has lateral pressure corresponding to 30−35 mN m^{-1},[43] we may infer from the results presented here that chitosan is likely to change the organization of membranes, especially by altering their viscoelastic properties. Indeed, according to Marsh,[43] the compressibility modulus (i.e., in-plane elasticity and dynamic elasticity) is the relevant quantity for the partitioning of molecules into the membrane or for conformational changes of proteins and polysaccharides at the membrane interface. Many proteins reduce membrane elasticity during insertion, though maintain the membrane structure.

(B) LB Films. In order to confirm the presence of chitosan on the interface at high surface pressures (such as 40 mN m^{-1}, close to collapse) and to look into the possibility of transferring the chitosan together with DMPA, we transferred pure DMPA and mixed chitosan−DMPA monolayers onto solid supports using the LB technique. Y-type LB films with up to 11 layers could be transferred for both DMPA and mixed chitosan−DMPA monolayers, with a transfer ratio of 1.05 ± 0.06 at a surface pressure of 40 mN m^{-1} and a chitosan concentration of 0.2 g L^{-1}. Figure 5 shows the nanogravimetry measurements taken with a QCM, and the mass was calculated by the Sauerbrey equation,[44] featuring an almost linear increase in mass with the number of layers. The mass per layer for pure DMPA LB films was 109.5 ng, while, for the mixed chitosan−DMPA, the mass

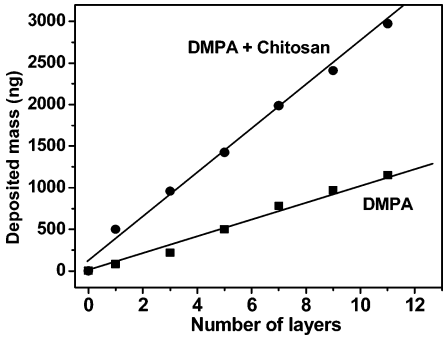

Figure 5. Nanogravimetry for DMPA LB films transferred from monolayers spread on the buffer with or without chitosan (0.2 g L^{-1}).

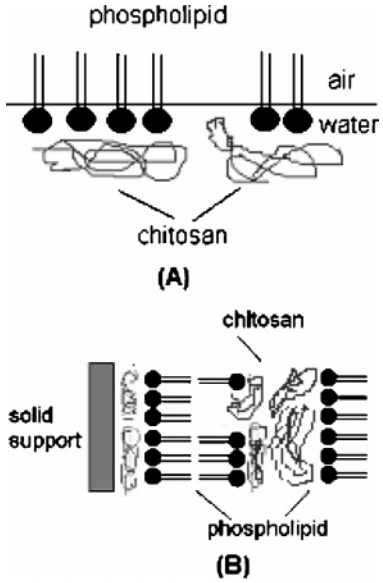

Figure 6. (A) Model for interaction of chitosan with lipids at the interface at high surface pressure values. (B) Scheme for mixed chitosan−DMPA LB films. In this model we consider neither the relative dimensions of the molecules, nor the aggregation and roughness of the films.

was 258.2 ng per layer. This 148.8 ng difference should be ascribed to chitosan adsorbed on the film.

It is believed that the interactions between chitosan and DMPA involves dipole and electrostatic interactions, with chitosan forming a subsurface. Hydrophobic interactions with chitosan (as suggested in a previous paper[40]) can also occur through acetyl groups, considering that it is reported in the literature on the formation of chitosan gels.[45] Also, we attested the decrease in surface tension for chitosan solutions in high concentrations (above 1 g/L); however, we have to emphasize that dipole and electrostatic interactions are in fact more relevant in this system.

According to the nanogravimetry results, chitosan was deposited in both downstrokes and upstrokes, thus forming a "bilayer" between two successive sheets of phospholipid (Figure 6 B). The area estimated for chitosan at each layer is ca. 4700 $Å^2$, considering the crystal area (0.384 cm^2) and numeric molecular weight of ca. 108 700. Although these values are close to layers with monomolecular thickness, we have to consider aggregation and roughness of the films (see further discussion for AFM data).

Figure 7 shows the FTIR spectra for 11-layer Y-type LB films from pure DMPA and mixed chitosan−DMPA. The main bands

(42) Ivanov, I. B.; Danov, K. D.; Ananthapadmanabhan, K. P.; Lips, A. *Adv. Colloid Interface Sci.* **2005**, *114*, 61−92.
(43) Marsh, D. *Biochim. Biophys. Acta: Biomembr.* **1996**, *1286*, 183−223.
(44) Sauerbrey, G. *Z. Phys.* **1959**, *155*, 206−222.
(45) Spinks, G. M.; Lee, C. K.; Wallace, G. G.; Kim, S. S. I.; Kim, S. J. *Langmuir* **2006**, *22*, 9375−9379.

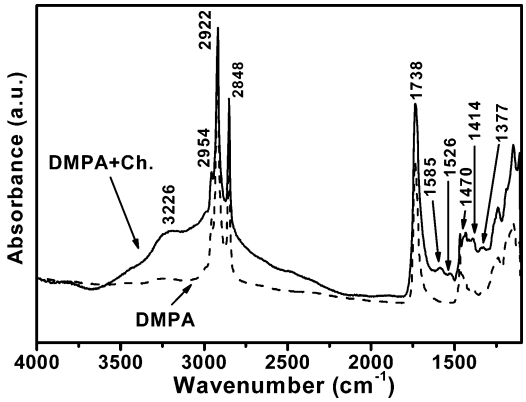

Figure 7. FTIR spectra for DMPA and mixed chitosan−DMPA LB films (11 layers for both cases).

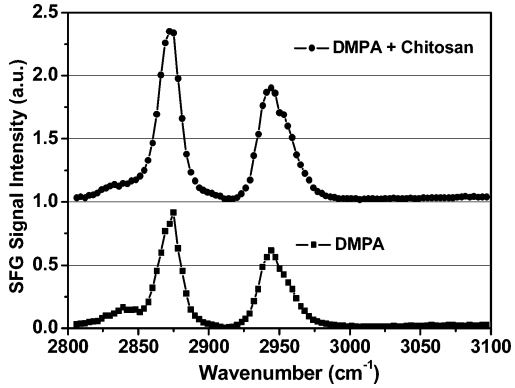

Figure 8. SFG spectra for one layer of DMPA or chitosan−DMPA LB film.

in the spectra are related to the phospholipid: 2954 cm^{-1} assigned to the asymmetric stretching mode of CH_3, and 2922 and 2848 cm^{-1} assigned to the asymmetric and symmetric stretching modes of CH_2. At lower wavenumbers, two bands appear at 1738 and 1470 cm^{-1} due to the stretching mode of the carboxyl group and scissor band of the CH_2, respectively. Also, the spectra show two small bands at 1414 and 1377 cm^{-1}, which may be due to the $\delta(CH_2)$ scissoring mode attached to the CO or PO groups and the $\delta(CH_3)$ umbrella mode, respectively. The spectra are consistent with those of Lozano et al.[46] For the chitosan-DMPA mixed film, a band appears centered at 3226 cm^{-1} assigned to the stretching of OH groups from chitosan. This band is broad because of hydrogen bonds or entrained water in the LB film.[47] The OH band overlaps the stretching band of NH. Two small bands are observed at 1585 and 1526 cm^{-1}, corresponding to NH deformation. These results confirm that chitosan must be at the interface even at high surface pressures in order to be transferred along with DMPA.

Figure 8 shows the SFG spectra for DMPA and mixed chitosan−DMPA monolayers displaying the CH-stretch bands for the films, which exist in both chitosan and DMPA. The spectra basically consist of two bands at ca. 2873 and 2944 cm^{-1} due to the CH_3 groups, corresponding to the CH symmetric stretch (r^+) and to its Fermi resonance with the overtone of CH_3 symmetric bending (r^+_{FR}), respectively.[32] A shoulder at ca. 2843 cm^{-1} is assigned to the symmetric stretch of methylene groups (d^+) and is only observed due to the presence of gauche defects in the alkyl chains, breaking the local symmetry for the

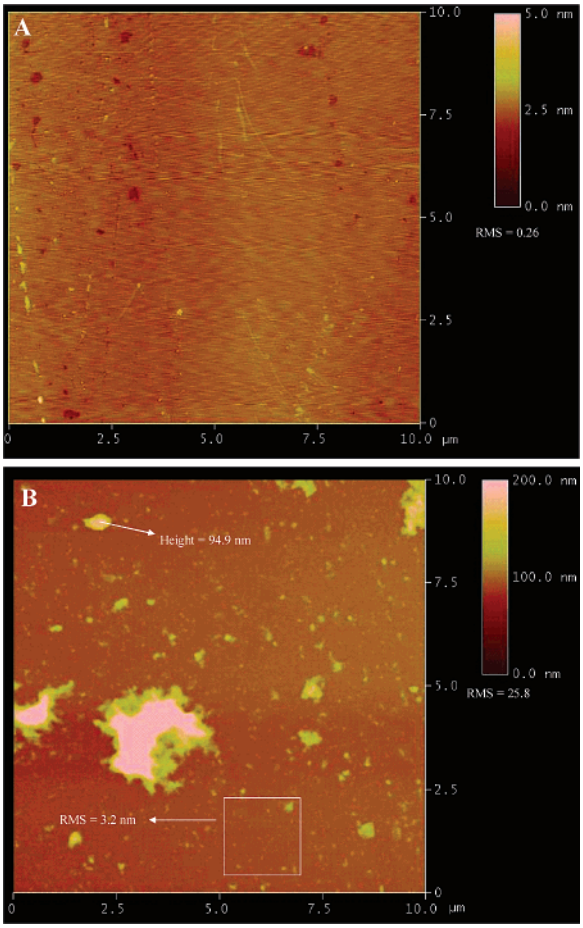

Figure 9. AFM images for one-layer LB films for DMPA (A) and chitosan−DMPA (B) monolayers transferred onto mica at 40 mN m^{-1}. The abbreviation rms refers to the root-mean-square roughness.

arrangement of CH_2 groups. Also, a shoulder at 2953 cm^{-1} (more evident for the mixed LB film) is due to the antisymmetric CH_3 stretch (r^-).

Since the spectra for pure DMPA and mixed DMPA−chitosan LB films are both quite similar, we conclude that no peaks were observed for chitosan, which means that chitosan molecules have a random conformation in the films. However, comparing the peak intensities in both spectra, we note that the r^+ peaks are stronger and the d^+ shoulder is weaker for mixed chitosan-DMPA monolayers, even with a lower lipid density in the film, because, at 40 mN m^{-1}, DMPA molecules occupy, on average, a larger molecular area (see Figure 1). This indicates that the close packing on both LB films is not sufficient to prevent gauche conformations in the lipid chains, but the average gauche defect density is lower in the mixed film, leading to an increased orientational ordering for the CH_3 groups of the phospholipid tails. These data are a strong indication that chitosan can enhance the alignment of DMPA chains.

The morphology of one-layer LB films is illustrated in the AFM images of Figure 9. Uniform LB films were obtained with pure DMPA, with a roughness of only 0.26 nm for a scanned area of 10 × 10 μm, which is consistent with the literature.[48] A completely different behavior was observed for the mixed chitosan−DMPA films, which were heterogeneous with large patches of chitosan (50−150 nm high). If such patches are considered in the roughness calculations, a value of 25.80 nm is obtained for a scanned area of 10 × 10 μm, as is the case in

(46) Lozano, P.; Fernandez, A. J.; Ruiz, J. J.; Camacho, L.; Martin, M. T.; Munoz, E. *J. Phys. Chem. B* **2002**, *106*, 6507−6514.

(47) Taboada, E.; Cabrera, G.; Cardenas, G. *J. Chil. Chem. Soc.* **2003**, *48*, 7−12.

(48) Souza, N. C.; Caetano, W.; Itri, R.; Rodrigues, C. A.; Oliveira, O. N.; Giacometti, J. A.; Ferreira, M. *J. Colloid Interface Sci.* **2006**, *297*, 546−553.

Table 2. Roughness and Thickness of LB Films Deposited from DMPA and Chitosan−DMPA Monolayers to Mica[a]

film	image dimension	roughness (rms) (nm)	thickness (nm)
DMPA 1 layer	10 μm	0.26	
	5 μm	0.22	1.7
	1 μm	0.20	
DMPA + chitosan 1 layer	10 μm	25.8	
	5 μm	39.0	5.8 − 47.8
	1 μm	12.1	

[a] The thickness for the mixed LB films was estimated in regions where there were no chitosan agglomerates.

Figure 9B. When regions of the film without the large patches were analyzed, the roughness was 3.16 nm for a scanned area of 2 × 2 μm, as shown in the inset of Figure 9B.

The larger roughness for the mixed films should be expected, as a similar behavior was observed for LB films of phospholipids containing proteins.[49] We also estimated the film thickness by measuring the depth profile across a furrow made in one-layer and five-layer LB films, according to the procedures of ref 30. The average thicknesses so obtained are given in Table 2, where DMPA films exhibited a thickness of 1.7 nm per layer, as expected,[47] while mixed chitosan−DMPA LB films displayed a thickness in the range between 5.8 and 47.8 nm per layer (taken on a region with no large chitosan patches). The lower limit is consistent with a monolayer of chitosan deposited underneath the DMPA layer, as suggested in the model in Figure 6. It is also consistent with the nanogravimetry results and the expectation of a thickness of 5−10 nm for a macromolecule with ca. 108 700 Da. The higher thicknesses indicate that, even in the regions with no clear patches, the chitosan layer is irregular, with aggregation. This agrees with Fang et al., who incubated chitosan in phospholipid bilayers supported on mica and demonstrated that chitosan aggregates in a lipid environment.[50] Also, the presence of chitosan aggregates confirm that chitosan molecules occupy a certain area at the interface, providing monolayer expansion and inducing the ordering of the DMPA chains, as demonstrated with SFG and surface potential measurements.

Conclusions

We have confirmed that chitosan can interact with lipid monolayers and adsorbs at the lipid monolayer even at high surface pressures, as shown in ref 40. Chitosan caused expansion of the monolayers, decreased the membrane elasticity, made the films heterogeneous, and enhanced the packing of the lipid chains. The results could be rationalized in terms of a model in which chitosan is located mainly as subsurface below the DMPA layer, interacting via dipole and electrostatic interactions. In addition, chitosan could be transferred onto solid supports with the LB technique, as demonstrated by FTIR and QCM measurements. Through AFM and SFG measurements in the LB films, we observed that chitosan caused marked changes in the structure and morphology of DMPA films, increasing their thickness and roughness and enhancing the chain ordering. The latter was consistent with an increased surface potential for the mixed chitosan−DMPA monolayer. These results may have important implications in the interaction of chitosan with biological membranes.

Acknowledgment. This work was supported by FAPESP, IMMP, FINEP, CNPq, and Rede Biomat (Brazil).

LA700856A

(49) Caseli, L.; Masui, D. C.; Furriel, R. P. M.; Leone, F. A.; Zaniquelli, M. E. D. *Thin Solid Films* **2007**, *515*, 4801−4807.

(50) Fang, N.; Chan, V. *Biomacromolecules* **2003**, *4*, 1596−1604.